Supplementary Fig. 1

A

Intestinal ATAC-seq Homer Motif p-value

	CDX2	HNF4A/G
	GCCATAAA	CAAAGTCC
E11.5	1e-1320	-
E14.5	1e-1198	1e-245
E16.5	1e-754	1e-1606
Adult	1e-295	1e-1418

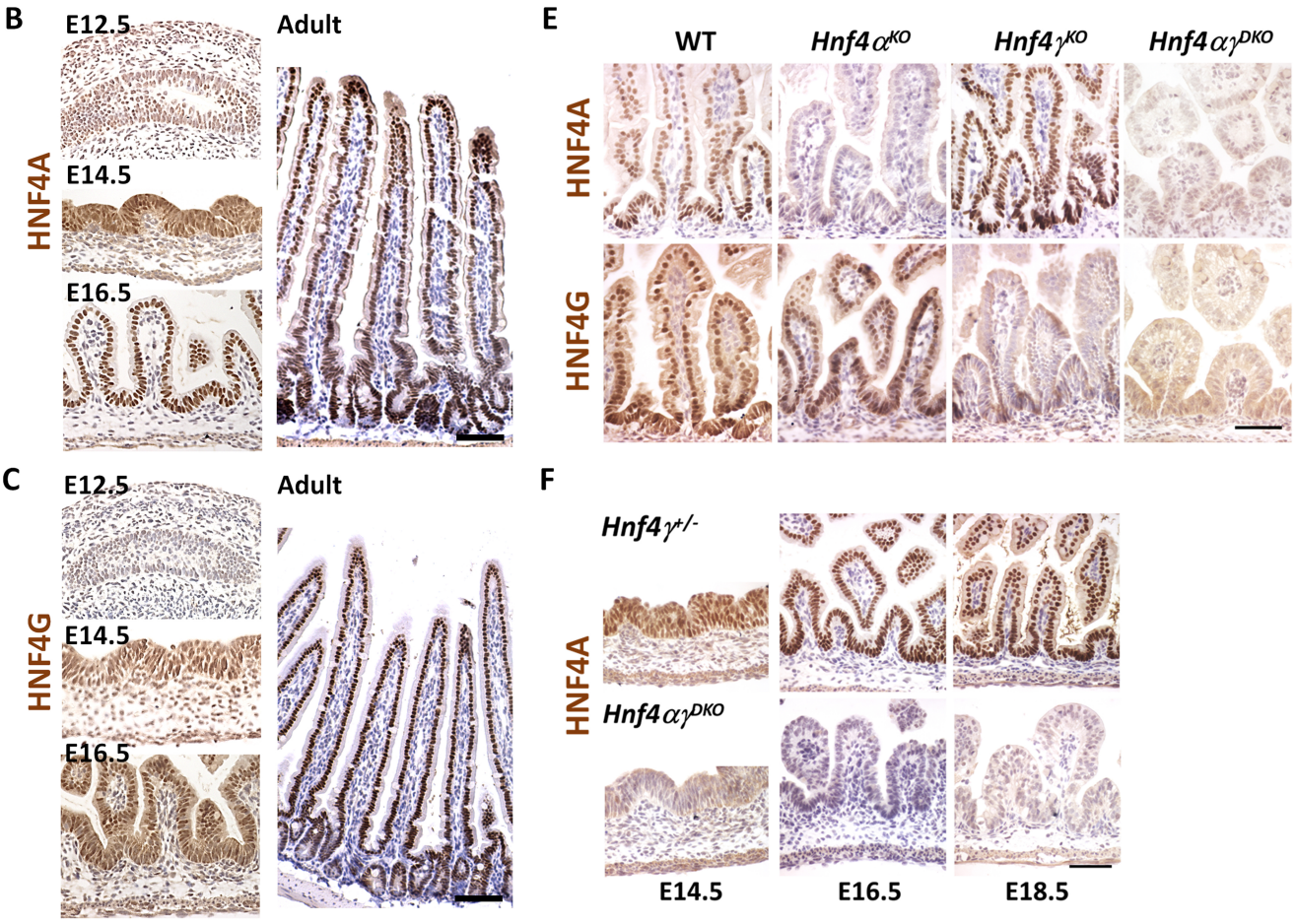

D

Fig. S1. HNF4 expression in the intestinal epithelium across developmental time. (A) HOMER *de novo* analysis of ATAC-seq (GSE115541, n = 2 biological replicates per timepoint, MACS *P* value $\leq 10^{-5}$) of mouse intestinal epithelial cells at each developmental time shows that CDX2 binding motifs are present as early as E11.5, whereas HNF4 binding motifs are not present until E14.5 (E11.5, E14.5 and E16.5: small intestinal epithelial cells; Adult: adult villus epithelial cells). HNF4 motifs are increasingly abundant at accessible regions as the intestine matures. Immunostaining of (B) HNF4A and (C) HNF4G shows that relative protein levels of these factors increase with developmental time in mouse (representative of 4 biological replicates, duodenum). (D) Schematic of human intestinal organoids differentiated from hESCs (Tsai et al., 2017). (E) HNF4A and HNF4G immunostaining shows loss of HNF4 in the E18.5 intestinal epithelium of both single and double mutants (representative of 4 biological replicates, E18.5 duodenum). (F) Immunostaining of HNF4A shows loss of HNF4A in the intestinal epithelium of E14.5 *Shh-Cre*$^{+}$ embryos *(*representative of 4 biological replicates, duodenum). Scale bars, 50 μm.

Supplementary Fig.2

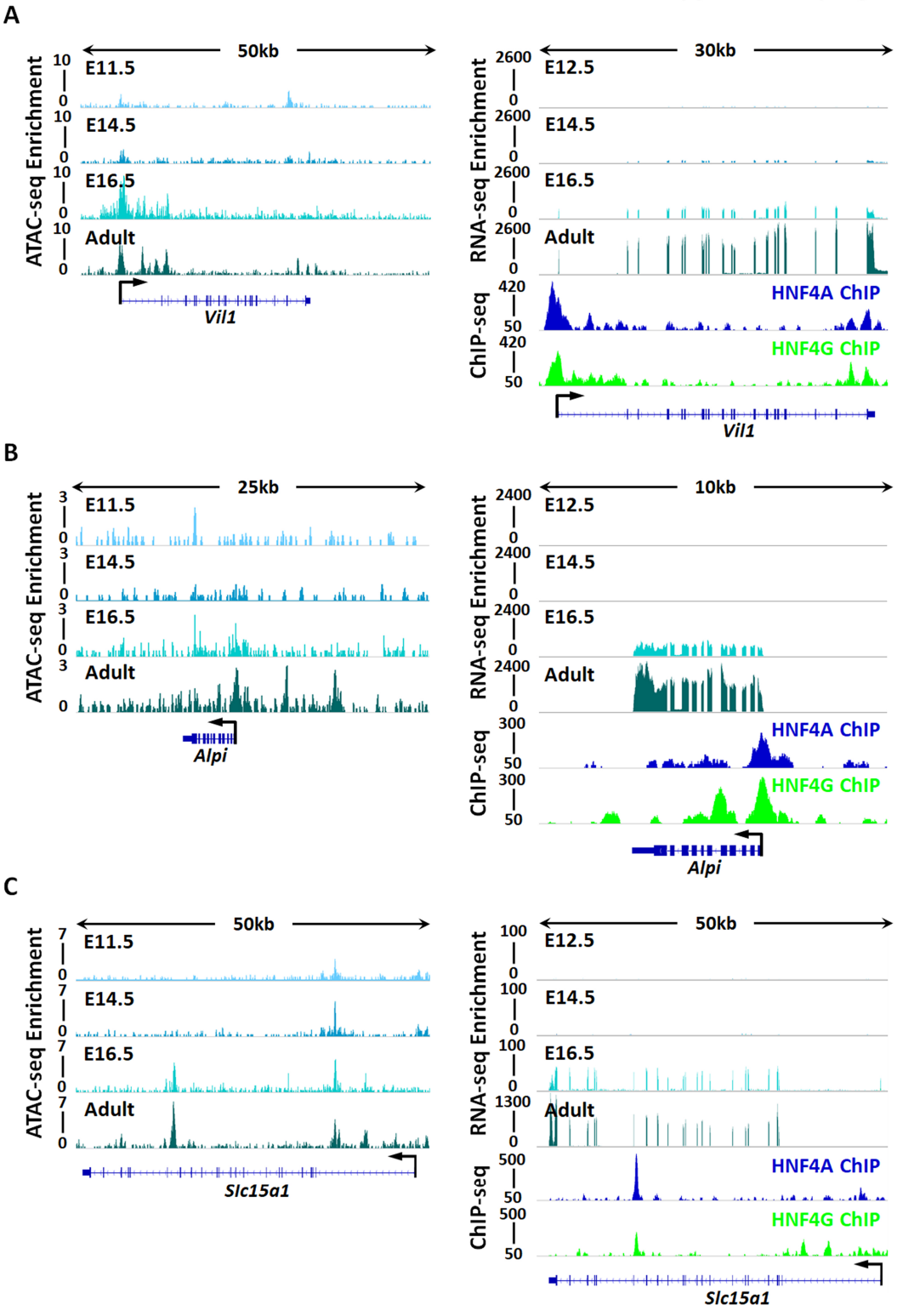

Fig. S2. HNF4 paralogs bind to and activate maturation-specific genes. Maturation-specific genes, such as (A) *Vil1*, (B) *Alpi* and (C) *Slc5a1*, show more accessible chromatin (ATAC-seq, left panels) and increased transcript levels (RNA-seq, right top panels) across developmental time, and HNF4 factors bind to the maturation-specific genes in the mature tissue of the adult (ChIP-seq, right bottom panels). n = 2 biological replicates per developmental timepoint for ATAC-seq (GSE115541), RNA-seq (GSE115541) and ChIP-seq (GSE112946).

Supplementary Fig. 3

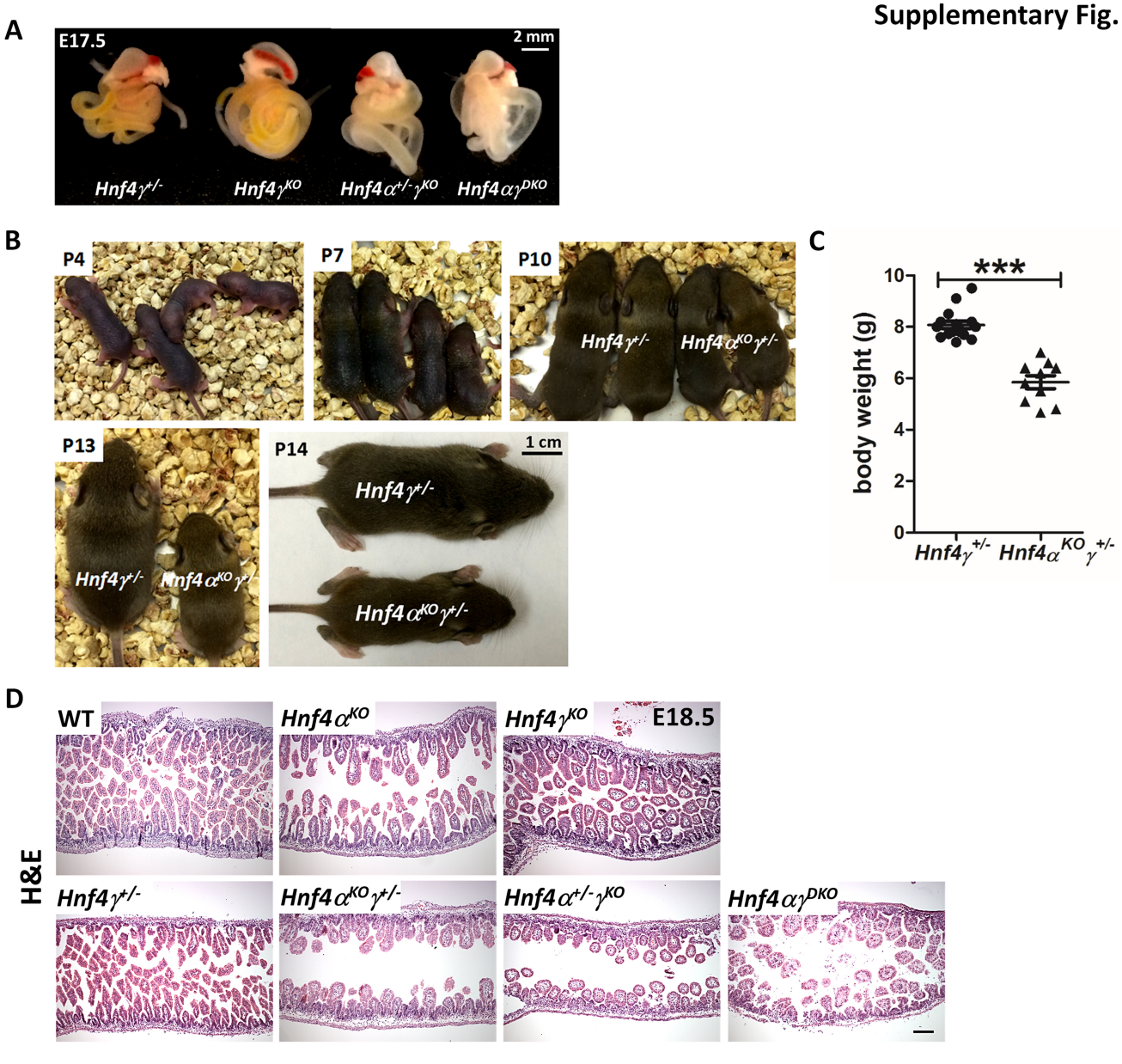

Fig. S3. Loss of 3 *Hnf4* alleles in the developing gut leads to growth retardation after birth. (A) Loss of 3 or 4 *Hnf4* alleles in developing embryos leads to an underdeveloped intestine with distended and translucent lumen (representative of 4 biological replicates). (B) $Hnf4\alpha^{KO}\gamma^{+/-}$ pups can survive after birth but show slower growth when compared to littermate controls. (C) Body weight of P14 pups. Data are presented as mean ± SEM ($Hnf4\gamma^{+/-}$ controls: n = 16; $Hnf4\alpha^{KO}\gamma^{+/-}$ mutants: n = 10; Student's t-test, two-sided at P < 0.001***). (D) *Hnf4* single mutants have a similar morphology to the controls, but loss of 3 or 4 *Hnf4* alleles in developing embryos leads to strikingly stunted villi, as evidenced by H&E staining (representative of 4 biological replicates, E18.5 duodenum; expanded panel from **Fig.6H**). Scale bars, 50 μm.

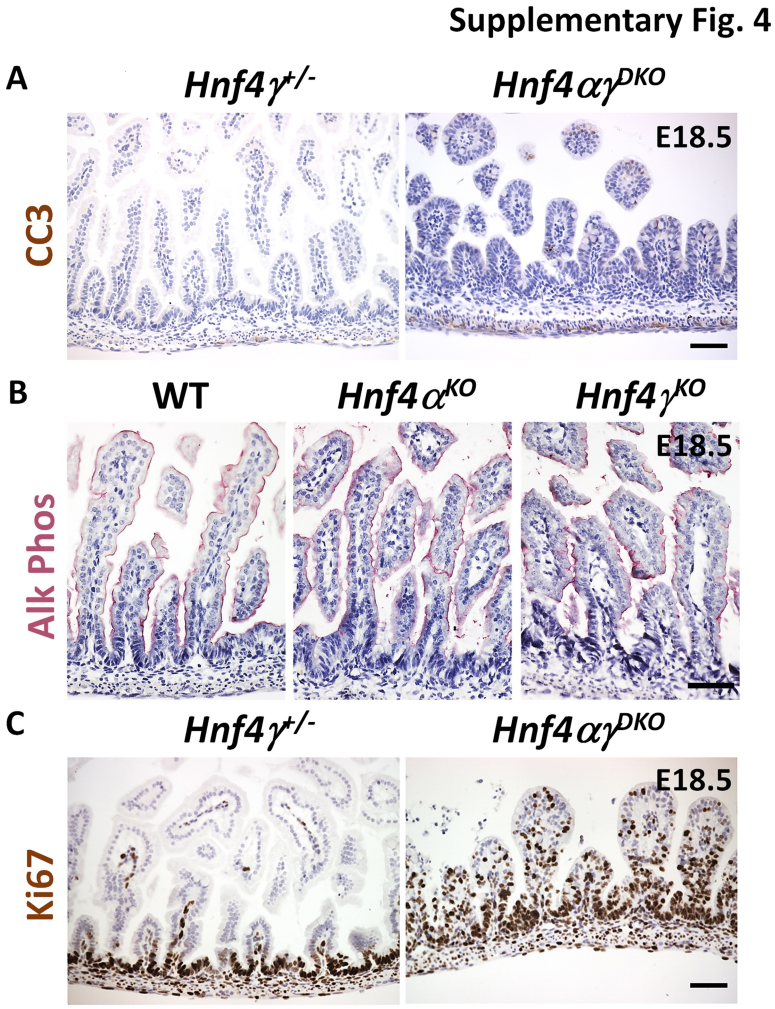

Fig. S4. Additional histological and immunochemical features of HNF4 mutant intestines. (A) *HNF4* mutants do not have significant cell death as shown in immunostaining of cleaved caspase 3 (representative of 4 biological replicates, E18.5 duodenum). (B) *Hnf4α*^{KO} and *Hnf4γ*^{KO} embryos do not have compromised intestinal maturation, as evidenced by alkaline phosphatase staining, indicating redundant roles for HNF4 factors in intestinal development (representative of 4 biological replicates, E18.5 duodenum). (C) Proliferative cells (Ki67^{+}) are observed in the villi of *Hnf4γα*^{DKO}, which may be due to compromised tissue maturation (representative of 4 biological replicates, E18.5 duodenum). Scale bars, 50 μm.

Supplementary information

Table S1. Genome coordinates for ATAC-seq performed in intestinal epithelial cells from E11.5 embryo to adult, including 30,702 embryonic enhancer regions (cluster 3 from **Fig.1A**) and 10,544 maturation enhancer regions (cluster 2 from **Fig.1A**). Additionally, the full list of HOMER *de novo* motif-calling analysis on these embryonic and maturation-enriched regions are reported respectively. Finally, the results of GO term enrichment using GREAT analysis for genes with their transcriptional start sites within 20 kb of these embryonic and maturation regions are reported respectively. These data correspond to findings in **Fig.1**.

Click here to Download Table S1

Table S2. ATAC-seq performed in intestinal epithelial cells from E16.5 Hnf4$\alpha\gamma^{DKO}$ versus Hnf4$\gamma^{+/-}$ controls. Genome coordinates for 5,391 accessible chromatin regions become inaccessible upon HNF4 loss (cluster 2 from **Fig.6A**). Additionally, the full list of HOMER *de novo* motif-calling analysis on these HNF4 chromatin-dependent regions are reported. Finally, the results of GO term enrichment using DAVID analysis for genes with their transcriptional start sites within 20 kb of these HNF4 chromatin-dependent regions are reported. GO and motif analysis of regions from cluster 3 of **Fig.6A** are also included. These data correspond to findings in **Fig.6**.

Click here to Download Table S2

Table S3. Details of sequencing data sets used in this study.

Click here to Download Table S3